

See discussions, stats, and author profiles for this publication at: <https://www.researchgate.net/publication/6144183>

# Self-assembled-monolayer-modified silicon substrate to enhance the sensitivity of peptide detection for AP-MALDI mass spectrometry

ARTICLE *in* JOURNAL OF MASS SPECTROMETRY · DECEMBER 2007

Impact Factor: 2.38 · DOI: 10.1002/jms.1261 · Source: PubMed

---

CITATIONS

17

---

READS

34

## 4 AUTHORS, INCLUDING:



[Shuchen Hsieh](#)

National Sun Yat-sen University

52 PUBLICATIONS 594 CITATIONS

SEE PROFILE



[Hui-Fen Wu](#)

National Sun Yat-sen University

176 PUBLICATIONS 2,191 CITATIONS

SEE PROFILE

# Self-assembled-monolayer-modified silicon substrate to enhance the sensitivity of peptide detection for AP-MALDI mass spectrometry

Shuchen Hsieh,\* Hsin-Yi Ku, Yao-Tang Ke and Hui-Fen Wu\*

Department of Chemistry and Center for Nanoscience and Nanotechnology, National Sun Yat-Sen University, 70 Lien-Hai Road, Kaohsiung, Taiwan 80424, Republic of China

Received 12 March 2007; Accepted 24 May 2007

A self-assembled-monolayer-modified silicon substrate was successfully used to enhance the sensitivity of peptide detection for atmospheric pressure-matrix-assisted laser desorption/ionization mass spectrometry (AP-MALDI/MS). The effect of surface modification of silicon wafer samples with  $\text{NH}_2$  and OH functional groups was investigated. In addition, solvent effects for the preparation of modified  $\text{NH}_2$ -functionalized surfaces were examined. The sensitivities for the two peptides were significantly improved, increasing between 12 and 160 times, for bradykinin and gramicidin, respectively, on an  $\text{NH}_2$ -modified silicon surface prepared in toluene, over that on a conventional gold substrate. The limits of detection (LODs) for bradykinin and gramicidin using the conventional gold substrate in AP-MALDI/MS experiments were  $>0.011\ \mu\text{M}$  and  $110\ \mu\text{M}$ , respectively. Using our SAM approach, the LODs for bradykinin and gramicidin in AP-MALDI/MS can be improved to  $0.93\ \text{nM}$  and  $0.33\ \mu\text{M}$ , respectively. This SAM approach for AP-MALDI/MS is simple and sensitive, and can be used for high-throughput analysis. Copyright © 2007 John Wiley & Sons, Ltd.

**KEYWORDS:** SAM substrate; AP-MALDI/MS; solvent effect; surface modification; self-assembled monolayer

## INTRODUCTION

Matrix-assisted laser desorption/ionization mass spectrometry (MALDI/MS) was discovered by Karas *et al.*<sup>1–4</sup> in the 1980s. This technique uses a laser excitation source to ionize particles in a substrate ‘matrix’. These particles then transfer charge to the molecules of interest through a proton transfer event, thus creating analyte ions. Because the proton transfer process requires only a single proton for each molecule, this is a soft ionization technique and has been largely used in the field of analytical biology.

Later in 1999, Wei *et al.*<sup>5</sup> improved the MALDI/MS technique by introducing a nonorganic matrix method. Wei used porous silicon as the substrate matrix and ‘bridge’ to absorb the ultraviolet laser energy, thus eliminating the need for an organic matrix such as  $\alpha$ -cyano-4-hydroxycinnamic acid (CHCA).<sup>6</sup> Because this technique requires only an inorganic porous silicon wafer substrate, the mass spectroscopy output is very clean, and contains information only from the compound of interest. Because silicon is a technologically important and widely available material, this new application has drawn much attention from many fields.

Self-assembled monolayers (SAMs) on silicon<sup>7–9</sup> have been studied since 1985, and are used in a great number

of important applications,<sup>10</sup> such as biosensors, molecular electronics, lubrication layers, corrosion protection, and nanocluster organization. More recently, these films have shown promise for enhancing the signal in MALDI/MS. The use of SAM-modified gold substrates for MALDI/MS has been demonstrated by several groups. Brockman *et al.*<sup>11</sup> have applied hydrophobic methyl-terminated SAM on a gold probe surface, and showed that the  $\text{CH}_3$ -SAM-modified gold surface was able to bind polypeptides via a hydrophobic interaction. Furthermore, the hydrophobic properties provided salt tolerance. Fukuo *et al.*<sup>12</sup> studied SAM of Ru complex on Au films. Stone *et al.*<sup>13</sup> used fluorinated SAMs to optimize the probe surface condition for matrix-assisted laser desorption ionization-ion mobility-surface-induced dissociation (MALDI-IM-SID). Min *et al.*<sup>14</sup> used maleimide-SAM on a modified Au surface to selectively immobilize cysteine-containing peptides. Mu *et al.*<sup>15</sup> studied low-density  $\text{COOH}$ -SAM on Au to selectively assemble the charged proteins, avidin, and streptavidin. Trauger *et al.*<sup>16</sup> showed that perfluorophenyl silylated and amine silylated porous silicon exhibit high sensitivity on Des-Arg-bradykinin and extend desorption/ionization on silicon mass spectrometry (DIOS-MS) activities to longer times.

For atmospheric pressure MALDI/MS (AP-MALDI/MS), many samples can be loaded simultaneously under atmospheric pressure, with each sample requiring an extremely short time for analysis. Therefore, it offers significant advantages over other methods by way of convenience, and rapid

\*Correspondence to: Shuchen Hsieh and Hui-Fen Wu, Department of Chemistry and Center for Nanoscience and Nanotechnology, National Sun Yat-Sen University, 70 Lien-Hai Road, Kaohsiung, Taiwan 80424, Republic of China.  
E-mail: shsieh@mail.nsysu.edu.tw; hfwu@mail.nsysu.edu.tw

and high-throughput analysis. However, this technique has been limited by poor sensitivity compared with conventional MALDI/MS operated in high vacuum. Thus, efforts to improve the sensitivity of AP-MALDI/MS are very important for further development of this recent technique. In this study, to the best of our knowledge, we have demonstrated for the first time the use of a SAM-modified unetched silicon wafer for AP-MALDI/MS to improve the sensitivity for two peptide samples. The effects of surface modification with  $\text{NH}_2$  and OH groups were investigated. In addition, solvent effects for the preparation of the  $\text{NH}_2$ -modified silicon samples were examined using bradykinin (1–8) and gramicidin as model compounds for this novel approach.

## EXPERIMENTAL

### Materials

Bradykinin fragment (1–8) (molecular weight 904 g/mol), gramicidin D (molecular weight 1882 g/mol), CHCA, and trifluoroacetic acid (TFA) were purchased from Sigma-Aldrich (St. Louis, MO, USA) and were used without further purification. Gramicidin has the amino acid sequence  $\text{HCO-L-Val}^1\text{-Gly}^2\text{-L-Ala}^3\text{-D-Leu}^4\text{-L-Ala}^5\text{-D-Val}^6\text{-L-Val}^7\text{-D-Val}^8\text{-L-Trp}^9\text{-D-Leu}^{10}\text{-L-Xxx}^{11}\text{-D-Leu}^{12}\text{-L-Trp}^{13}\text{-D-Leu}^{14}\text{-L-Trp}^{15}\text{-NHCH}_2\text{CH}_2\text{OH}$ , where Xxx<sup>11</sup> is Trp in gramicidin A, Phe in gramicidin B, and Tyr in gramicidin C. The commercial gramicidin D contains a mixture of 80, 5, and 15 parts of the components A, B, and C, respectively. Toluene, acetone, and (3-aminopropyl) triethoxysilane (APTES) were purchased from Mallinckrodt (Phillipsburg, NJ, USA). Methanol was purchased from Echo Chemical Co. Ltd. Water used for sample preparation was purified using a Milli-Q reagent water treatment system (Millipore, Milford, MA, USA).

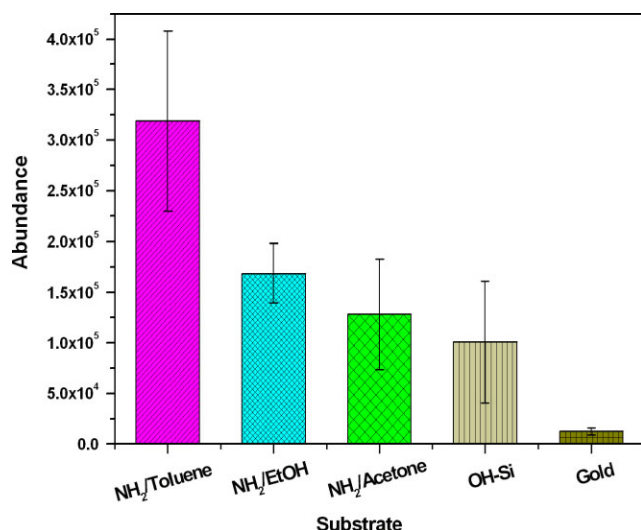


**Figure 1.** Bradykinin (1–8) fragment abundance from MALDI mass spectra for several  $\text{NH}_2$ -terminated SAM modified Si(100) substrates, an OH-rich Si(100) substrate, and a standard gold substrate. A total volume of 2  $\mu\text{l}$  of 11 nM bradykinin solution were deposited on each substrate for MALDI analysis. The  $\text{NH}_2/\text{Toluene}$  combination provided the best and most repeatable signal and was used exclusively for all subsequent experiments.

### Sample preparation

Matrix solution was prepared using CHCA, which was dissolved in a 1% solution of TFA in methanol/water (2:1, v/v). Stock standard solutions of bradykinin fragment (1–8) and gramicidin were prepared in methanol and stored in a refrigerator at 4 °C.

### Instrumentation

#### AP-MALDI/MS

All AP-MALDI/MS experiments were conducted using a Finnigan LCQ ion trap mass spectrometer (Thermoquest Inc., San Jose, CA, USA) equipped with a commercial AP-MALDI source (Mass Tech., Columbia, MD, USA). A nitrogen laser with a UV wavelength of 337 nm was used for all experiments. The laser power was attenuated to 60% at 10 Hz repetitions. CHCA was used as the MALDI matrix. Mass spectra were obtained in the positive ion mode. All mass spectra were generated using 3-min laser shots. The ion injection time was 1070 ms; capillary temperature 250 °C; capillary voltage 40 V; and tube lens offset voltage 70 V. The target plate bias was 1.8 kV. Standard gold and SAM-modified silicon substrates were attached to the target plate with double-sided carbon tape (Ted Pella, Inc.). Two microliters of the matrix (CHCA) solution was added by means of the 'dried droplet' method. Samples were air-dried for 5 min at room temperature and then loaded into the AP-MALDI/MS for analysis.

#### FTIR

Fourier transform infrared spectroscopy (FTIR) data for the  $\text{NH}_2$ -modified silicon substrates was acquired using a Spectrum 100 FTIR Spectrometer (PerkinElmer) equipped

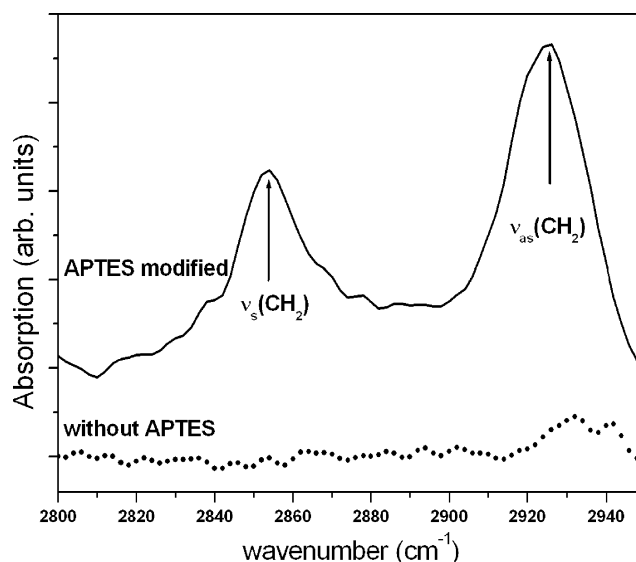


**Figure 2.** FTIR spectra for the  $\text{NH}_2$ -terminated SAM-modified Si(100) substrate and a clean silicon sample. The peaks correspond to the  $\text{CH}_2$  symmetric and  $\text{CH}_2$  asymmetric stretch positions reported in the literature.<sup>17</sup> The control sample was also treated with toluene to rule out contamination as the source of the  $\text{CH}_2$  peaks. Thus, the presence of  $\text{CH}_2$  stretching peaks confirms the growth of the APTES SAM on the Si surface.

with a liquid nitrogen-cooled mercury cadmium telluride (MCT) detector. Transmitted signal was used to detect molecular-level signal on the silicon surface.<sup>17</sup> The incident light was oriented along the surface normal, and spectra were collected over 1000 scans at a resolution of  $8\text{ cm}^{-1}$ . A background spectrum from a freshly cleaned silicon substrate was collected before each measurement.

### AFM

Topographic images of the samples were obtained using an atomic force microscope (AFM) (Asylum Research MFP-3D, Santa Barbara, CA, USA) operating in intermittent contact mode under ambient conditions. A silicon cantilever (Olympus, AC240) with a nominal spring constant of  $1\text{ N/m}$  was used for all images with a scan rate of  $1.0\text{ Hz}$  and image pixel density of  $512 \times 512$ .

### Preparation of SAM-modified silicon substrate

Self-assembled monolayers were prepared on Si(100) substrates using a solution mixture of APTES, and anhydrous ethanol, toluene, or acetone. The Si(100) wafers were first cleaned using a micro surfactant followed by an ethanol rinse, and then dried under a stream of dry nitrogen gas. These wafers were then treated using a plasma cleaner (Harrick Scientific Products, Inc.) for 2 min to increase the OH concentration at the surface. Several methods for preparing  $\text{NH}_2$ -modified Si(100) substrates have been reported in the literature,<sup>18–20</sup> each with its own solvent mixture. We have used three of these to prepare samples in this study in order to identify the optimal preparation method for use in the MALDI/MS technique. In the first method, a plasma-cleaned, OH-rich silicon substrate was immersed in a solution of APTES/anhydrous ethanol ( $v/v = 1:20$ ) for 12 h<sup>18</sup> and then removed and dried under a stream of dry nitrogen gas. For the second method, the OH-rich Si(100) substrate was immersed in a solution of  $5.0 \times 10^{-3}\text{ M}$  APTES in a solvent mixture of acetone and ultra pure water ( $v/v = 5:1$ ) for 12 h<sup>20</sup> and then removed and dried under a stream of dry nitrogen gas. For the third method, the OH-rich Si(100) substrate was immersed in a solution of 1% APTES in toluene for 12 h.<sup>19</sup> Following this, the sample was removed from the solution and baked in an oven at  $120^\circ\text{C}$  for 5 min.

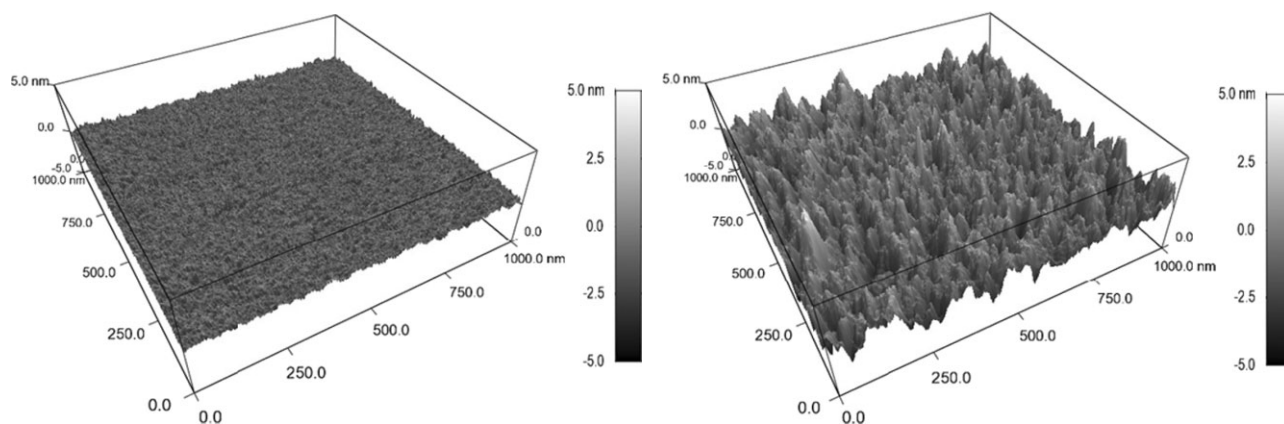
## RESULTS AND DISCUSSION

### Effect of surface modification with $\text{NH}_2$ and OH, and solvent effects

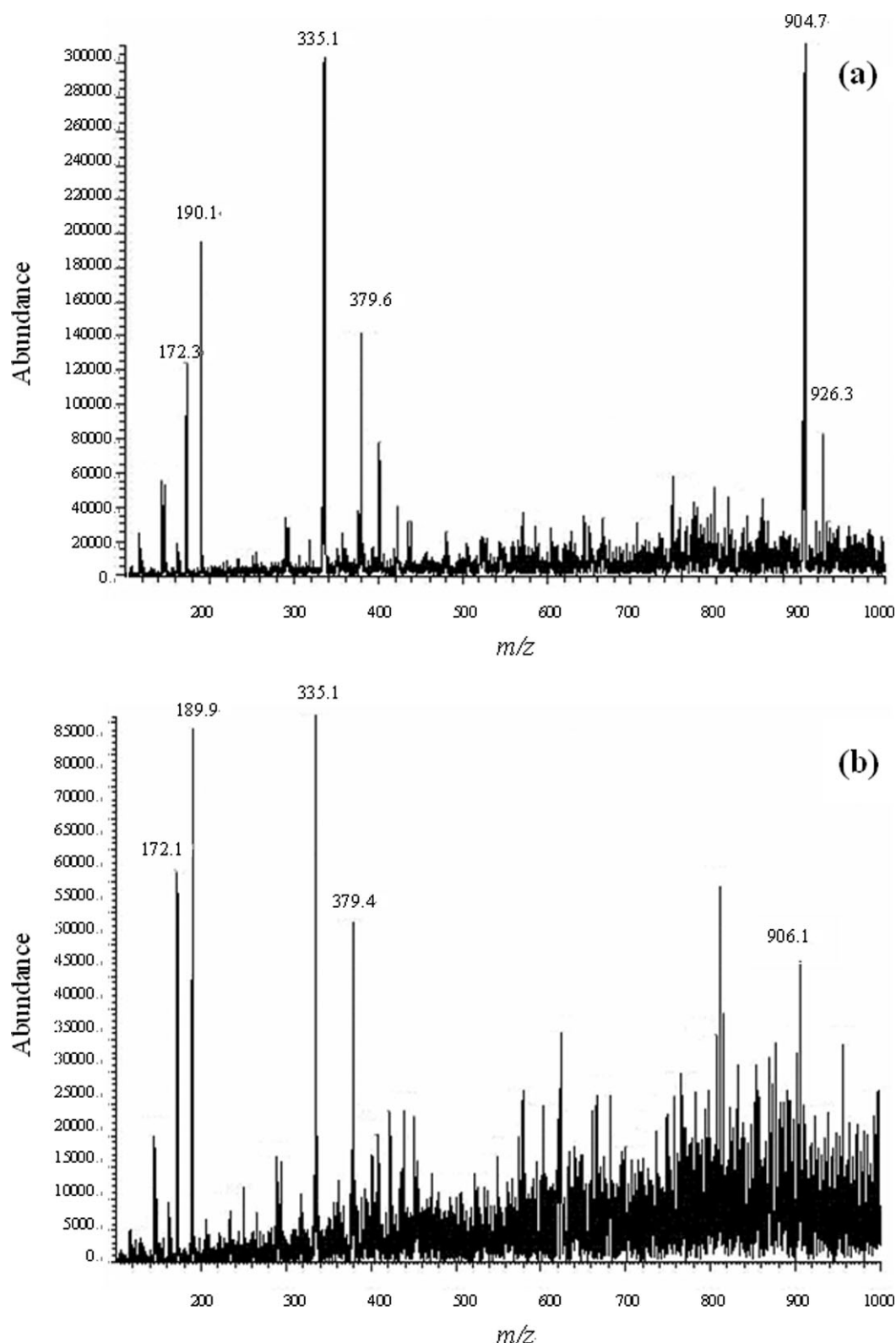
In order to investigate the solvent effect, (APTES) SAM-modified Si(100) samples were prepared using toluene, acetone, and ethanol prior to the addition of the bradykinin (1–8) or the gramicidin samples. The AP-MALDI results from these substrates were then compared with the results for samples prepared using the same concentrations of analyte on conventional gold substrate samples. In addition, the effect of the chemically functionalized surface, both  $\text{NH}_2$ - and OH-modified silicon wafer samples, were examined.

Figure 1 shows the AP-MALDI/MS ion abundance results for bradykinin (1–8) fragment deposited on  $\text{NH}_2$ -terminated SAM modified Si(100) substrates prepared from three different solvents, an OH-rich Si(100) substrate, and a standard gold substrate. A total volume of  $2\text{ }\mu\text{L}$  of  $0.011\text{ }\mu\text{M}$  bradykinin solution was deposited on each substrate for AP-MALDI analysis. Six samples of each substrate were analyzed and averaged. The AP-MALDI/MS ion abundance results for  $\text{NH}_2$ /toluene,  $\text{NH}_2$ /ethanol,  $\text{NH}_2$ /acetone, OH-Si, and gold, were  $319\,094 \pm 89\,013$ ,  $168\,834 \pm 29\,313$ ,  $128\,122 \pm 54\,789$ ,  $101\,080 \pm 60\,238$  and  $12\,687 \pm 3502$ , respectively. Most notably, all the samples prepared using silicon showed higher ion abundance than the standard gold substrate. Of the silicon samples, the one prepared using an APTES/toluene solvent mixture gave the highest signal in the AP-MALDI/MS data, and was used exclusively for all subsequent experiments. The OH-Si substrate exhibited much lower abundance than that of any of the  $\text{NH}_2$ -SAM-modified silicon samples. This indicates that the SAM layer plays an important role in enhancing ion abundances for bradykinin (1–8).

The  $\text{NH}_2$ -modified silicon samples, prepared using the APTES/toluene mixture, were further characterized using FTIR spectroscopy in order to confirm the presence of an  $\text{NH}_2$ -terminated SAM monolayer. The specific method we used involved mounting the Silicon sample such that the incident IR beam was along the surface normal and the transmitted light (through the silicon sample) was



**Figure 3.** AFM topographical image (a) of an OH-modified silicon surface. The root mean square (RMS) roughness for the entire imaged area was  $0.19\text{ nm}$ . AFM topographical image (b) of  $\text{NH}_2$ -modified silicon surface. The RMS roughness for the entire imaged area was  $1.05\text{ nm}$ . Both images correspond to  $1\text{ }\mu\text{m} \times 1\text{ }\mu\text{m}$ .



**Figure 4.** (a) Plot of MALDI mass spectra abundance versus  $m/z$  for a bradykinin solution concentration of 11 nM on the  $\text{NH}_2$ -terminated SAM Si(100) substrate. Figure (b) shows the corresponding MALDI spectrum for an 11 nM (the detection limit) bradykinin sample on a gold standard substrate.

monitored using an MCT detector. This method is a useful tool for characterizing SAM film growth on silicon substrates.

The portion of the spectrum corresponding to the  $\text{CH}_2$  symmetric and asymmetric stretching modes ( $\nu_{\text{as}}(\text{CH}_2)$  and

$\nu_{\text{s}}(\text{CH}_2)$ ) is shown in Fig. 2. The dashed line represents the FTIR signal from a blank Si(100) sample that was immersed in pure toluene without APTES. This data is included to rule out contamination as the source of the  $\text{CH}_2$  stretching signal in the APTES sample FTIR result. The  $\text{CH}_2$  peaks were used

rather than the  $\text{NH}_2$  peak to confirm the SAM film growth because of the small signal of  $\text{NH}_2$  at  $\sim 3200\text{--}3500\text{ cm}^{-1}$  (only one moiety per APTES molecule) and its overlap with the  $\text{H}_2\text{O}$  peak, which is present in the background. The positions of the two  $\text{CH}_2$  peaks in the spectrum at  $2854$  and  $2927\text{ cm}^{-1}$ , corresponding to the  $\nu_s(\text{CH}_2)$  and  $\nu_{as}(\text{CH}_2)$  stretch respectively, are in agreement with literature values<sup>21,22</sup> and confirm the presence of APTES on the silicon surface.

Another important characteristic of the sample substrates is the surface roughness, which may influence the binding affinity of analytes (bradykinin (1–8) or gramicidin) to the SAM surfaces. We have used AFM to characterize the surface roughness of an OH-rich Si(100) and an  $\text{NH}_2$ -terminated SAM on Si(100) surface. The resulting topographical images are shown in Fig. 3. In order to compare the relative surface features between these samples, we have displayed the images ( $1\text{ }\mu\text{m} \times 1\text{ }\mu\text{m}$ ) in a 3D projected view format using the same  $10\text{ nm}$  Z scale. Qualitatively, the OH-modified silicon surface appears to be smoother than the  $\text{NH}_2$ -modified Si(100) surface. The root mean square (RMS) roughness for the two substrates, OH and  $\text{NH}_2$  was  $0.19$  and  $1.05\text{ nm}$ , respectively. Although we cannot rule it out, the increased roughness of the  $\text{NH}_2$ -SAM substrate does not account for the degree of signal enhancement observed by us. Okuno *et al.*<sup>23</sup> showed that roughness at the submicron scale, not the nanometer scale, was the key factor in improving the ionization efficiency for hydrophilic polymers on scratched silicon and stainless steel samples using matrix-free MALDI. Thus, we believe that chemical differences in the films rather than the small physical differences (roughness) result in the enhanced AP-MALDI/MS signal for bradykinin.

Figure 4(a) shows the AP-MALDI mass spectrum for a  $0.011\text{ }\mu\text{M}$  concentration of bradykinin (1–8) on an  $\text{NH}_2$ -SAM-modified silicon wafer formed using toluene as the solvent. A total volume of  $2\text{ }\mu\text{L}$  of bradykinin (1–8) solution was deposited on an area of the sample, roughly  $5\text{ mm} \times 5\text{ mm}$ , corresponding to an adsorbed surface concentration of  $4.2 \times 10^{-4}$  bradykinin (1–8) molecules/ $\text{nm}^2$  (or  $420$  molecules/ $\mu\text{m}^2$ ). The protonated bradykinin (1–8) molecule shown at  $m/z$   $904.7$  ( $[\text{M} + \text{H}]^+$ ) in Fig. 4(a) is present at an abundance of  $\sim 300\,000$ . Figure 4(b) shows the AP-MALDI mass spectrum for a bradykinin (1–8) sample on a conventional gold substrate using the same concentration and preparation procedure as for the modified Si substrate. The protonated bradykinin (1–8) molecule at  $m/z$   $904.7$  ( $[\text{M} + \text{H}]^+$ ) was not detected and only the background noise (CHCA matrix ions) was observed in the spectra. This is because the limits of detection (LOD) of bradykinin (1–8) on a conventional Au substrate is higher than  $0.011\text{ }\mu\text{M}$ .

#### Determination of sensitivity for $\text{NH}_2$ -modified silicon surface prepared in toluene for bradykinin (1–8)

A significant signal enhancement for bradykinin (1–8) was observed in AP-MALDI/MS when it was deposited on  $\text{NH}_2$ -modified silicon surfaces compared to deposition on a conventional gold substrate. In order to determine the LOD

for this approach, we selected the APTES/toluene mixture to prepare a set of  $\text{NH}_2$ -SAM-modified silicon substrates as it exhibited the highest sensitivity in our solvent effects results (Fig. 1). A series of samples with different concentrations of bradykinin (1–8) were prepared and their AP-MALDI mass spectra were collected. These results are shown in Fig. 5.

As shown in Fig. 4(a), the detection limit of bradykinin on a conventional gold substrate is  $>0.011\text{ }\mu\text{M}$ . For the same bradykinin concentration on an  $\text{NH}_2$ -modified Si substrate, we observed a signal of  $\sim 2.8 \times 10^5$  which corresponds to an enhancement of  $\sim 20\times$  over the standard gold substrate. Further measurements were made (Fig. 5) by diluting the bradykinin (1–8) solutions in order to determine the detection limit for bradykinin on the  $\text{NH}_2$ -modified Si substrate. Six samples at each concentration were analyzed and the results averaged. The AP-MALDI/MS ion abundance results for concentrations of  $0.93$ ,  $1.4$ ,  $2.8$ ,  $5.5$ , and  $11\text{ nM}$ , were  $29\,052 \pm 14\,820$ ,  $44\,622 \pm 14\,801$ ,  $60\,072 \pm 13\,240$ ,  $203\,445 \pm 103\,873$  and  $319\,094 \pm 89\,013$ , respectively. At a concentration of  $0.93\text{ nM}$  of bradykinin solution, one can see in the figure that the signal is at the detection limit. This amounts to a lowering of the detection limit of bradykinin by nearly 12 times using our  $\text{NH}_2$ -SAM-modified silicon samples prepared in toluene over that on conventional Au substrates.

#### Determination of sensitivity for $\text{NH}_2$ -modified silicon surface prepared in toluene for the hydrophobic peptide gramicidin D

A second peptide, gramicidin D, was used to further test the  $\text{NH}_2$ -SAM-modified silicon samples prepared in toluene to determine if the enhanced AP-MALDI/MS signal could be observed for a hydrophobic peptide, since it is extremely difficult to detect hydrophobic peptides using conventional gold substrates in AP-MALDI/MS. Gramicidin is a linear polypeptide antibiotic, containing 15 amino acids (D and L forms) with an ethanolamine residue at the carboxyl end and a formyl group at the amino end. All the side chains on gramicidin are relatively hydrophobic.<sup>24–27</sup>

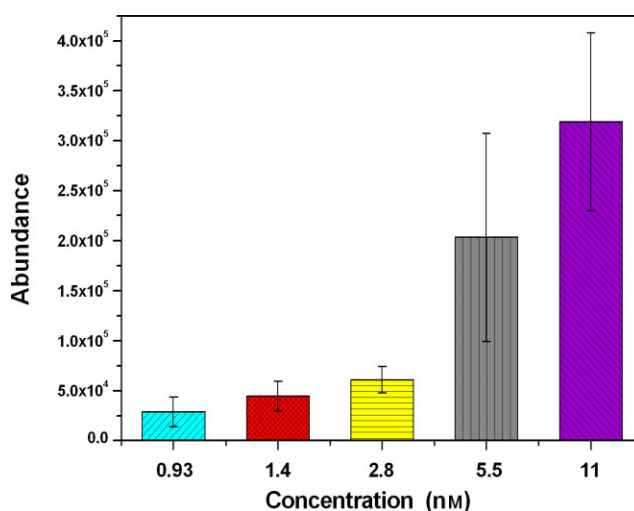


**Figure 5.** MALDI abundance versus bradykinin concentration on the  $\text{NH}_2$ -terminated SAM prepared using the APTES/toluene mixture on Si.

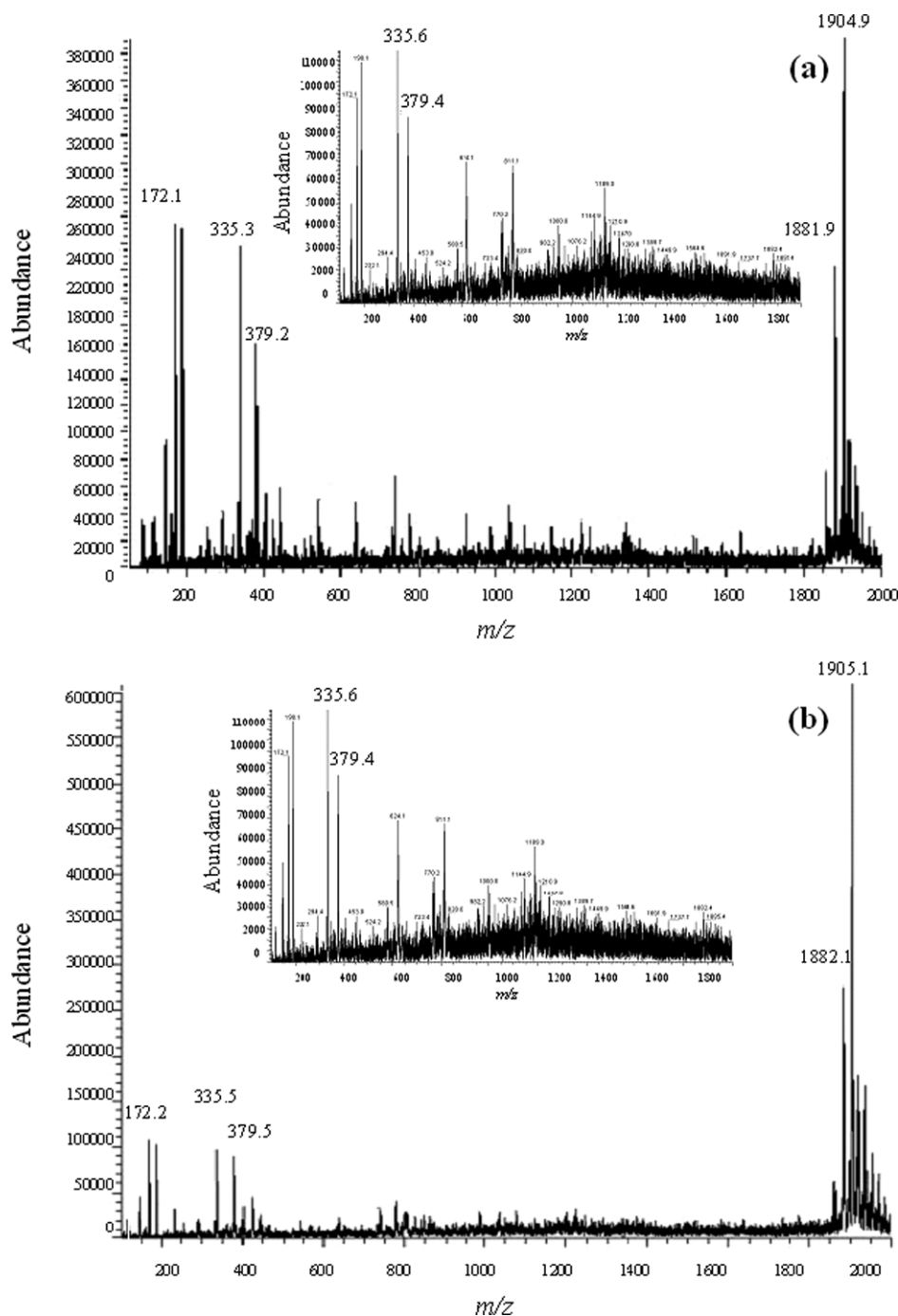


**Figure 6.** MALDI mass spectra of gramicidin deposited on  $\text{NH}_2$ -terminated SAM-modified Si(100) substrates: (a) 13  $\mu\text{M}$ , (b) 2.7  $\mu\text{M}$ , (c) 1.3  $\mu\text{M}$ , (d) 0.33  $\mu\text{M}$ . The 0.33  $\mu\text{M}$  concentration represents a 160 $\times$  reduction in the detection limit on this substrate compared to the standard gold substrate (54  $\mu\text{M}$ ) shown in the inserts.

Gramicidin was deposited on  $\text{NH}_2$ -SAM-modified Si(100) substrates prepared in toluene and AP-MALDI mass spectra were subsequently acquired. These results were also compared with those obtained using conventional gold substrates at the same gramicidin concentration. Figure 6(a–d) shows AP-MALDI mass spectra collected for four different gramicidin concentrations. The concentrations in Fig. 6(a–d) were 13, 2.7, 1.3, and 0.33  $\mu\text{M}$  with corresponding ion abundance signals of 255 100, 284 638, 345 232 and 119 721, respectively. Since the LOD for gramicidin was 110  $\mu\text{M}$  using a conventional gold substrate, all the insert figures in

Fig 6(a–d) show those spectra obtained from conventional gold substrates using the same concentration of gramicidin. Only the matrix ions of CHCA can be seen in these data. Here, even though gramicidin D was used, its primary component (80% gramicidin A) was the dominant form detected by us and was observed as protonated ion and sodium ion adducts. The product ions shown at  $m/z$  1882 and 1905 are identified as  $[\text{Val-GrA} + \text{H}]^+$ ,  $[\text{Val-GrA} + \text{Na}]^+$ , respectively.

The ion abundance from AP-MALDI/MS *versus* gramicidin concentration is plotted in Fig. 7. Six samples at

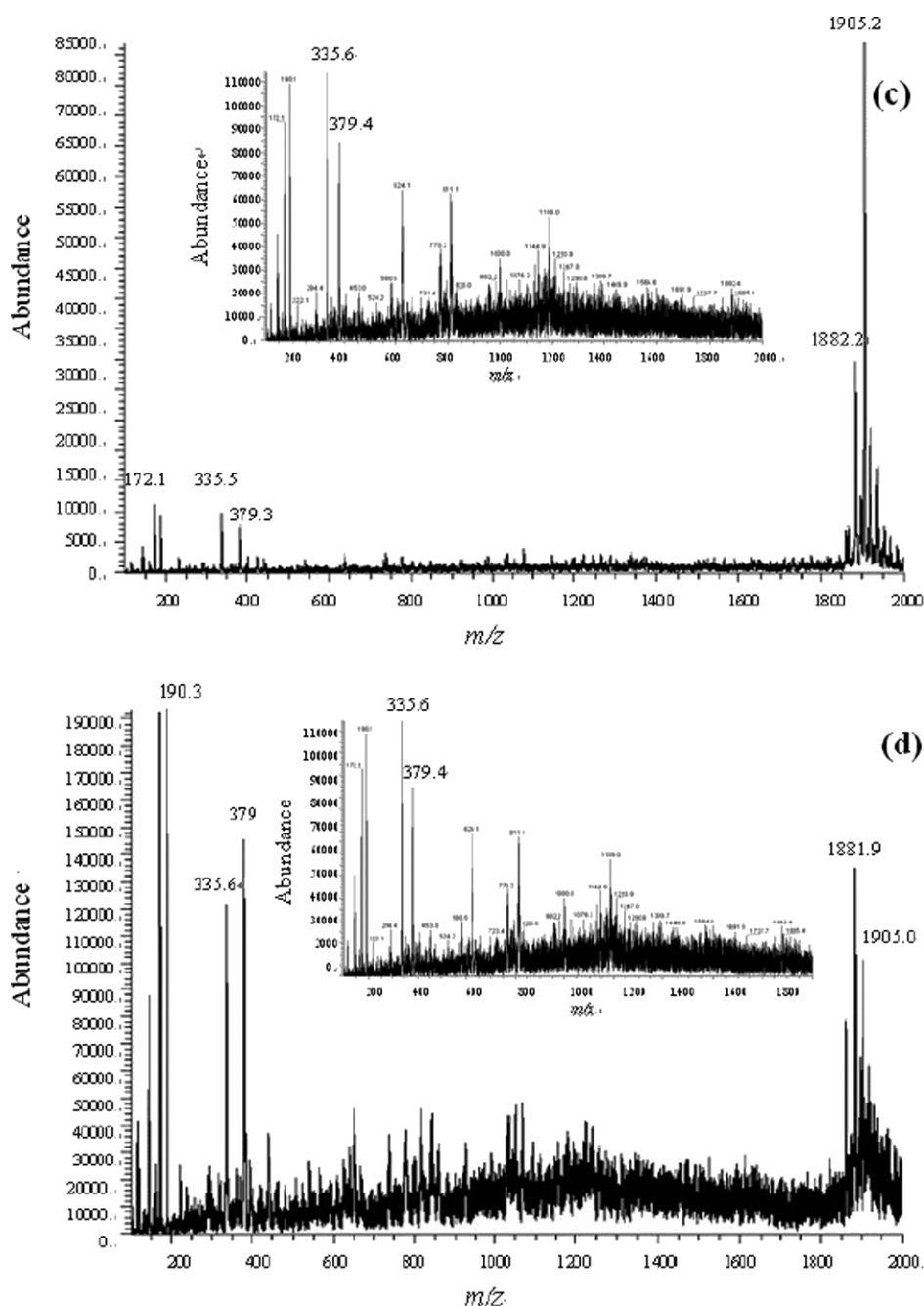


Figure 6. (Continued).

each concentration were analyzed and averaged. The AP-MALDI/MS ion abundance results for concentrations of 0.33, 0.67, 1.3, 2.7, 13, and 27  $\mu\text{M}$  were  $119721 \pm 31267$ ,  $75557 \pm 34885$ ,  $345232 \pm 80754$ ,  $284638 \pm 67271$ ,  $255100 \pm 81453$ , and  $170010 \pm 66879$ , respectively.

As shown in Fig. 7, there is a maximum in the AP-MALDI abundance for a 1.3  $\mu\text{M}$  concentration of gramicidin. The abundance decreases for both higher and lower gramicidin concentrations. A possible explanation for this is when concentrations are higher than 1.3  $\mu\text{M}$ , gramicidin that agglomeration leads to stronger gramicidin–gramicidin interactions which reduce the overall AP-MALDI/MS signal. For concentrations lower than 1.3  $\mu\text{M}$ , there is simply less gramicidin on the surface resulting in a lower

signal. The lowest gramicidin concentration used in this study was 0.33  $\mu\text{M}$ , corresponding to a surface density of  $1.27 \times 10^{-2}$  molecules/ $\text{nm}^2$  for gramicidin. This concentration represents the detection limit for gramicidin on the  $\text{NH}_2$ -SAM-modified Si(100) substrates used in this study. Furthermore, this shows a reduction in detection limit of 160 fold over that for gramicidin deposited on a conventional gold substrate (54  $\mu\text{M}$ ). When compared with the bradykinin results, the dramatic enhancement in sensitivity of AP-MALDI/MS observed for gramicidin deposited on  $\text{NH}_2$ -terminated SAM-modified Si(100) substrates prepared in toluene has demonstrated that this approach is useful, especially for the detection of hydrophobic proteins.



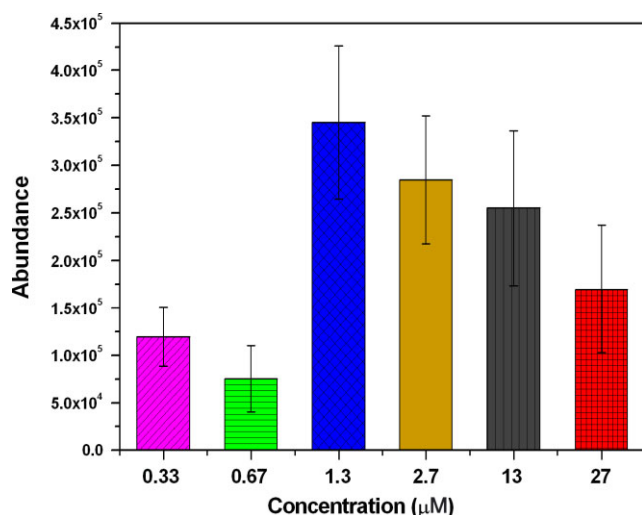


**Figure 7.** MALDI abundance versus gramicidin concentration on the NH<sub>2</sub>-terminated SAM prepared using the APTES/toluene mixture on Si. The signal increases as the concentration decreases from 27 to 1.3 μM and then decreases as the concentration is further reduced to 0.33 μM. This behavior is discussed in the text.

## CONCLUSIONS

We have demonstrated that the sensitivity of AP-MALDI/MS can be significantly enhanced, and detection limits can be greatly reduced by using an NH<sub>2</sub>-terminated SAM-modified Si(100) substrate prepared in toluene. For bradykinin, the detection limit was lowered by a factor of 12, and for gramicidin, a 160-fold reduction was observed. The reason for this improvement is attributed to the SAM layer, which provides a more efficient pathway for energy transfer to the peptide molecules resulting in higher sensitivity in AP-MALDI/MS. This simple SAM approach has the potential to make a great impact on the development of AP-MALDI/MS, making it a more rapid, sensitive, and higher-throughput analysis tool.

## Acknowledgements

The authors thank National Science Council (NSC 95-2113-M-110-019-MY3) of Taiwan and National Sun Yat-sen University for financial support of this work. Shuchen Hsieh would like to thank David Beck for helpful discussions. Hui-Fen Wu thanks the National Science Council of Taiwan for supporting the three-year projects under the contract numbers NSC 92-2113-M-032-015, NSC 93-2113-M-032-014, and NSC 94-2113-M-110-117 to purchase the LCQ.

## REFERENCES

1. Karas M, Bachmann D, Hillenkamp F. Influence of the wavelength in high-irradiance ultraviolet-laser desorption mass-spectrometry of organic-molecules. *Analytical Chemistry* 1985; **57**: 2935.
2. Karas M, Bachmann D, Hillenkamp F. Matrix-assisted ultraviolet-laser desorption of nonvolatile compounds. *International Journal of Mass Spectrometry* 1987; **78**: 53.
3. Karas M, Hillenkamp F. Laser desorption/ionization of proteins with molecular masses exceeding 10000 daltons. *Analytical Chemistry* 1988; **60**: 2299.
4. Tanaka K, Waki H, Ido Y, Akita S, Yoshida Y, Yoshida T. Protein and polymer analyses up to *m/z* 100,000 by laser ionization

time-of-flight mass spectrometry. *Rapid Communications in Mass Spectrometry* 1988; **2**: 151.

5. Wei J, Buriak JM, Siuzdak G. Desorption-ionization mass spectrometry on porous silicon. *Nature* 1999; **399**: 243.
6. Laiko VL, Moyer SC, Cotter RJ. Atmospheric pressure MALDI/Ion trap mass spectrometry. *Analytical Chemistry* 2000; **72**: 5239.
7. Allara DL, Nuzzo RG. Spontaneously organized molecular assemblies. 1. Formation, dynamics, and physical properties of *n*-alkanoic acids adsorbed from solution on an oxidized aluminum surface. *Langmuir* 1985; **1**: 45.
8. Allara DL, Nuzzo RG. Spontaneously organized molecular assemblies. 2. Quantitative infrared spectroscopic determination of equilibrium structures of solution-adsorbed *n*-alkanoic acids on an oxidized aluminum surface. *Langmuir* 1985; **1**: 52.
9. Wasserman SR, Whitesides GM, Tidswell IM, Ocko BM, Pershan PS, Axel JD. The structure of self-assembled monolayers of alkylsiloxanes on silicon: a comparison of results from ellipsometry and low-angle X-ray reflectivity. *Journal of the American Chemical Society* 1989; **111**: 5852.
10. Ulman A. Formation and structure of self-assembled monolayers. *Chemical Reviews* 1996; **96**: 1533.
11. Brockman AH, Dodd BS, Orlando R. A desalting approach for MALDI-MS using on-probe hydrophobic self-assembled monolayers. *Analytical Chemistry* 1997; **69**: 4716.
12. Fukuo T, Monjushiro H, Hong H, Haga M, Arakawa R. Matrix-assisted laser desorption/ionization time of flight mass spectrometry of self-assembled monolayers of ruthenium complexes on gold. *Rapid Communications in Mass Spectrometry* 2000; **14**: 1301.
13. Stone EG, Gillig KJ, Ruotolo BT, Russell DH. Optimization of a matrix-assisted laser desorption ionization-ion mobility-surface-induced dissociation-orthogonal-time-of-flight mass spectrometer: simultaneous acquisition of multiple correlated MS1 and MS2 spectra. *International Journal of Mass Spectrometry* 2001; **212**: 519.
14. Min D-H, Yeo W-S, Mrksich M. A method for connecting solution-phase enzyme activity assays with immobilized format analysis by mass spectrometry. *Analytical Chemistry* 2004; **76**: 3923.
15. Mu L, Liu Y, Zhang S, Liu B, Kong J. Selective assembly of specifically charged proteins on an electrochemically switched surface. *New Journal of Chemistry* 2005; **29**: 847.
16. Trauger SA, Go EP, Shen Z, Apon JV, Compton BJ, Bouvier ESP, Finn MG, Siuzdak G. High sensitivity and analyte capture with desorption/ionization mass spectrometry on silylated porous silicon. *Analytical Chemistry* 2004; **76**: 4484.
17. Sambasivan S, Hsieh S, Fischer D, Hsu SM. Effect of SAM film order on nanofriction using NEXAFS. *Journal of Vacuum Science and Technology A* 2006; **124**: 1484.
18. Hsieh S, Meltzer S, Wang CRC, Requicha AAG, Thompson ME, Koel BE. Imaging and manipulation of gold nanorods with an atomic force microscope. *Journal of Physical Chemistry B* 2002; **106**: 231.
19. Masuda Y, Jinbo Y, Yonezawa T, Koumoto K. Templated site-selective deposition of titanium dioxide on SAM. *Chemistry of Materials* 2002; **14**: 1236.
20. Ren S, Yang S, Zhao Y. Micro- and macro-tribological study on a self-assembled dual-layer film. *Langmuir* 2003; **19**: 2763.
21. Kurth DG. Surface reactions on thin layers of silane coupling agents. *Langmuir* 1993; **9**: 2965.
22. Nakanishi K, Solomon P. *Infrared Absorption Spectroscopy*. San Francisco: Holden-Day, 1977.
23. Okuno S, Arakawa R, Okamoto K, Matsui Y, Seki S, Kozawa T, Tagawa S, Wada Y. Requirements for laser-induced desorption/ionization on submicrometer structures. *Analytical Chemistry* 2005; **77**: 5364.
24. Chen Y, Tucker A, Wallace BA. Solution structure of a parallel left-handed double-helical gramicidin-A determined by 2D <sup>1</sup>H NMR. *Journal of Molecular Biology* 1996; **264**: 757.

25. Sudhir P-R, Wu H-F, Zhou Z-C. An application of electrospray ionization tandem mass spectroscopy to probe the interaction of Ca/Mg/Zn and Cl<sup>-</sup> with gramicidin A. *Rapid Communications in Mass Spectrometry* 2005; **19**: 1517.
26. Urry DW. The Gramicidin A transmembrane channel: a proposed ( $\pi$ ) helix. *Proceedings of the National Academy of Sciences of the United States of America* 1971; **68**: 672.
27. Veatch WR, Fossel ET, Blout ER. The conformation of gramicidin A. *Biochemistry* 1974; **13**: 5249.